

University of Bologna Report  
DFUB 01/01

MACRO AND THE ATMOSPHERIC NEUTRINO PROBLEM

M. SPURIO for the MACRO collaboration <sup>a</sup>

*Dipartimento di Fisica dell'Università and INFN, 40126 Bologna, Italy*  
*e-mail: spurio@bo.infn.it*

After a brief presentation of the MACRO detector we discuss the updated data on atmospheric muon neutrinos, and the interpretation in terms of neutrino oscillations.

## 1 Introduction

MACRO is a multipurpose underground detector designed to search for rare events in the cosmic radiation. It performs measurements in areas of astrophysics, nuclear, particle and cosmic ray physics. In this paper we shall discuss the measurement of the atmospheric muon neutrino flux in the energy region from a few GeV up to a few TeV, and the interpretation of the MACRO results in terms of neutrino oscillations. The detector has global dimensions of  $12 \times 9.3 \times 76.5$  m<sup>3</sup> and provides a total acceptance to an isotropic flux of particles of  $\sim 10,000$  m<sup>2</sup> sr. The total mass is  $\simeq 5300$  t. A cross section of the detector is shown in Fig. 1a<sup>1</sup>. It has three sub-detectors: liquid scintillation counters, limited streamer tubes and nuclear track detectors. The mean rock depth of the overburden is  $\simeq 3700$  m.w.e. The average residual energy and the muon flux at the lab depth are  $\sim 310$  GeV and  $\sim 1$  m<sup>-2</sup> h<sup>-1</sup>, respectively.

## 2 MACRO as atmospheric $\nu_\mu$ detector

Primary cosmic rays produce in the upper atmosphere pions and kaons, which decay,  $\pi \rightarrow \mu\nu$ ,  $K \rightarrow \mu\nu$ ; and  $\mu \rightarrow e\nu_e\nu_\mu$ . Fig. 1a shows the three different topologies of neutrino events detected by MACRO: up throughgoing muons<sup>2</sup>, semicontained upgoing muons (IU) and up stopping muons + semicontained downgoing muons (UGS + ID)<sup>3</sup>. The parent  $\nu_\mu$  energy spectra for the three event topologies were computed with Monte Carlo (MC) methods, and presented in Fig. 1b. The number of events measured and expected for the three topologies is given in Table 1. Sources of background and systematic effects were studied in detail in<sup>3,4</sup> and found to be negligible. The neutrino energies involved in all event topologies are such that the  $\mu_\nu$  flux is up-down symmetric.

**High energy sample.** The *up throughgoing muons* come from  $\nu_\mu$ 's interacting in the rock below the detector; they are identified using the streamer tube system (for tracking) and the scintillator system (for time-of-flight (ToF)

---

<sup>a</sup>Invited talk at the Third International Workshop on New Worlds in Astroparticle Physics 1-3 September 2000, University of the Algarve. Faro, Portugal

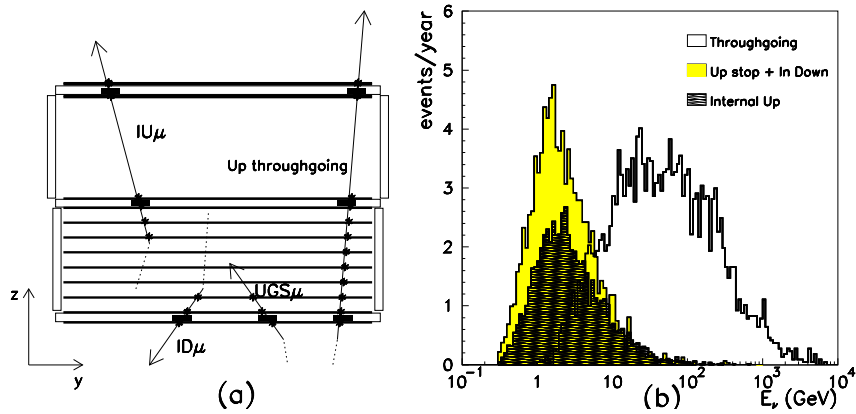


Figure 1: a) Event topologies induced by  $\nu_\mu$  interactions in and around MACRO. The black boxes are scintillator hits. The track direction and versus are measured by the streamer tubes and time of flight. b) Neutrino energy distribution for the three event topologies detected by MACRO

	Events selected	Predictions No oscil.	R = Data/MC
Up throughgoing	723	989	$0.731 \pm 0.028_{st}$ $\pm 0.044_{sys} \pm 0.124_{th}$
Internal Up	135	245	$0.55 \pm 0.04_{st}$ $\pm 0.06_{sys} \pm 0.14_{th}$
UpG Stop + In Down	229	329	$0.70 \pm 0.04_{st}$ $\pm 0.07_{sys} \pm 0.18_{th}$

Table 1: Event summary for the MACRO atmospheric neutrino flux analyses. The data correspond to a lifetime of  $\sim 5$  y with the full detector, after background corrections [2,3]. The ratios  $R = \text{Data/MC}$  are relative to MC expectations assuming no oscillations.

measurement). A rejection factor of at least  $10^5$  is needed in order to separate the up-going muons from the large background of down-going muons<sup>2</sup>. The  $\nu_\mu$  median energy is  $\overline{E}_\nu \sim 50$  GeV, and muons with  $E_\mu > 1$  GeV cross the whole detector. Fig. 2a shows the zenith angle distribution of the measured flux of up throughgoing muons. The data have been compared with MC simulations<sup>2</sup>; the expected angular distributions for no oscillations is shown in Fig. 2a as a dashed line, and for a  $\nu_\mu \rightarrow \nu_\tau$  oscillated flux with  $\sin^2 2\theta = 1$  and  $\Delta m^2 = 0.0025$  eV<sup>2</sup>, as a solid line. The total theoretical uncertainty on the expected muon flux, adding in quadrature the errors from neutrino flux, cross section and muon propagation, is 17 %; it is mainly a scale error that does not change the shape of the angular distribution. The ratio of the observed

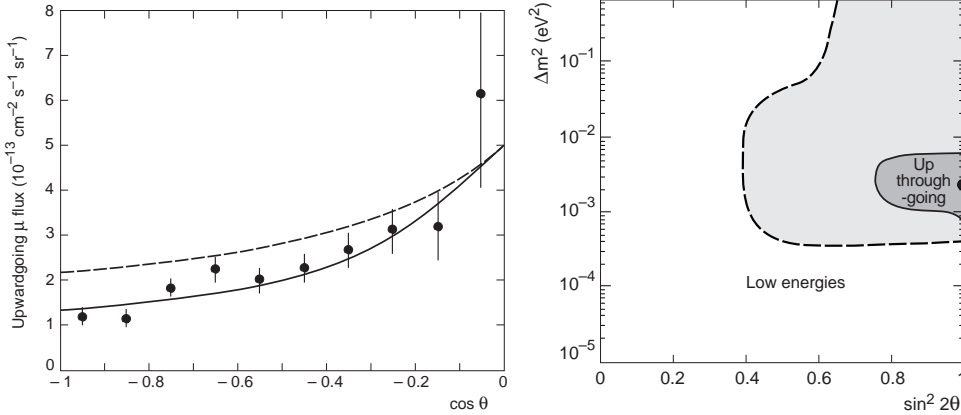


Figure 2: (a) Measured flux (points) of the up throughgoing muons plotted vs. zenith angle  $\Theta$ . The solid line is the fit to an oscillated muon flux, obtaining maximum mixing and  $\Delta m^2 = 0.0025 \text{ eV}^2$ . (b) Confidence regions for  $\nu_\mu \rightarrow \nu_\tau$  oscillations at the 90 % CL, obtained from MACRO high energy [2] and low energy [3] data.

number of events to the expectation without oscillations is given in Table 1.

**Low energy samples.** The *upgoing semicontained muons* (IU, in Fig. 1a) come from  $\nu_\mu$  interactions inside the lower apparatus. Since two scintillation counters are intercepted, the ToF is applied to identify the upward going muons. The average parent neutrino energy for these events is 4.2 GeV. The *upgoing stopping muons* (UGS) are due to external  $\nu_\mu$  interactions yielding upgoing muon tracks stopping in the detector; the *semicontained downgoing muons* (ID) are due to  $\nu_\mu$  induced downgoing tracks with vertices in the lower MACRO. The events were selected by means of topological criteria; the lack of time information prevents to distinguish the two sub samples, for which an almost equal number of events is expected. The average neutrino energy for these events is  $\simeq 3.5 \text{ GeV}$ . The number of events and the angular distributions are compared with the predictions<sup>3</sup> in Fig. 3 and Table 1.

### 3 Interpretation in terms of neutrino oscillations

We interpreted the reduction on the detected number of events (Table 1) and the deformation of the zenith angle distribution of the up-throughgoing events (Fig. 2a) as a consequence of  $\nu_\mu$  disappearance.

The weak flavor eigenstates ( $\nu_e, \nu_\mu, \nu_\tau$ ) are relevant for the production of atmospheric neutrinos, via  $\pi \rightarrow \mu\nu_\mu$ ,  $\text{K} \rightarrow \mu\nu_\mu$  and  $\mu \rightarrow e\nu_e\nu_\mu$  decays. For massive neutrinos one has to consider the mass eigenstates ( $\nu_1, \nu_2, \nu_3$ ) which are relevant for propagation. The flavor eigenstates are linear combinations of the mass eigenstates,  $\nu_l = \sum_{m=1}^3 U_{lm}\nu_m$ . In the simplest two flavors oscillations scenario, only one mixing angle  $\theta$  is involved, and the rate of  $\nu_\mu$  disappearance is given by

$$P(\nu_\mu \rightarrow \nu_\mu) \simeq 1 - \sin^2 2\theta \sin^2(1.27\Delta m^2 L/E_\nu) \quad (1)$$

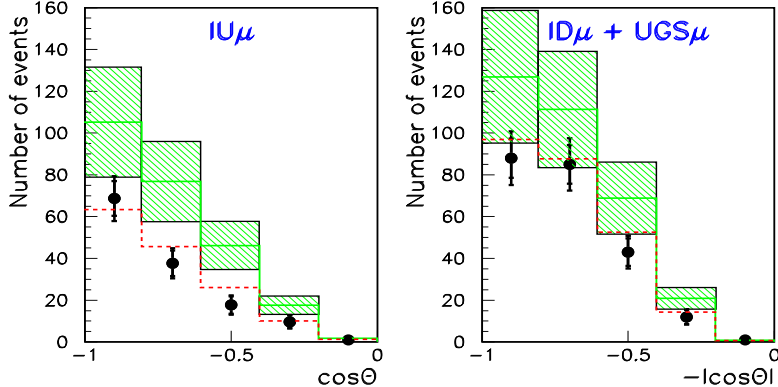


Figure 3: Measured (points) and expected number of low energy muon neutrino events versus zenith angle. IU: up semicontained. ID+UGS: up stopping plus down semicontained muons. The shadowed regions are the predictions without oscillations; the dotted lines are the predictions assuming neutrino oscillations with the parameters obtained from the up throughgoing sample.

$\Delta m^2 = m^2_{\nu_3} - m^2_{\nu_2}$ ,  $L$  = distance (in km) from the decay point to the interaction point,  $E_\nu$  is the neutrino energy, in GeV.

This simple relation could be modified when neutrinos propagate with a flavor-dependent interaction through matter<sup>5</sup>. This case is important, because the *matter effect* could help to discriminate between  $\nu_\mu$  oscillation in different neutrino channels. The matter effect in the Earth could enhance (in a range of values of the oscillations parameters) the  $\nu_\mu$  disappearance effect through "resonances" (MSW effect). This happens only for  $\nu_\mu \rightarrow \nu_e$  and for  $\nu_\mu \rightarrow \nu_s$  channels ( $\nu_s = \text{sterile neutrino}$ ), while for  $\nu_\mu \rightarrow \nu_\tau$  there is no matter effect ( $\nu_\mu$  and  $\nu_\tau$  have the same weak potential).

In the scenario described by eq. 1, relatively fewer up throughgoing muons are expected near the vertical ( $\cos\Theta = -1$ ) than near the horizontal ( $\cos\Theta = 0$ ), due to the longer path length of neutrinos from production to observation, in a wide range of  $\Delta m^2$  values. The probabilities to obtain the number of events in Table 1 and the angular distribution observed in Fig. 2a have been calculated *vs.* oscillation parameter values. For  $\nu_\mu \rightarrow \nu_\tau$  oscillations the maximum probability is 57 %, for  $\Delta m^2 = 0.0025 \text{ eV}^2$ ,  $\sin^2 2\theta = 1$  (combination from the shape of the angular distribution and the reduction in the number of events). Fig. 2b shows the 90 % CL regions for  $\nu_\mu \rightarrow \nu_\tau$ .

The probability for no-oscillations is 0.4%. The maximum probability for  $\nu_\mu \rightarrow \nu_s$  oscillations is 15%. Another way to discriminate between the  $\nu_\mu$  oscillation in  $\nu_\tau$  or in  $\nu_s$  is to study the angular distribution in two bins. The statistical significance is higher<sup>6</sup> with respect to the 10-bins fit of the angular distribution. From this ratio, the  $\nu_\mu \rightarrow \nu_s$  hypothesis is disfavored at level of 2.5 $\sigma$  compared to  $\nu_\mu \rightarrow \nu_\tau$ <sup>5</sup>.

From our results on the high energy sample, a  $\sim 50\%$  reduction in the flux of the up stopping events (UGS) as well of semicontained upgoing muons (IU) is expected, with no distortion in the shape of the angular distribution. No reduction is instead expected for the semicontained downgoing events (ID, coming from neutrinos with path lengths of  $\sim 15$  km). This is what is observed in Fig. 3. The allowed region in the  $\Delta m^2, \sin^2 2\theta$  plane is shown in Fig. 2b.

#### 4 Up throughgoing muon energy separation

The up throughgoing muon sample is induced by atmospheric  $\nu_\mu$  in a wide energy range (for 90% of events  $5 \lesssim E_\nu \lesssim 700$  GeV, and  $2 \lesssim E_\mu \lesssim 300$  GeV, see Fig. 1b). If the observed event reduction is due to neutrino oscillations, the first minimum of eq. 1 occurs at  $E_\nu \simeq 10 - 30$  GeV (for neutrinos from the nadir direction and oscillation parameters in the range of Fig. 2b). Thus, the  $\nu_\mu$  disappearance mechanism works on (relatively) lower energy neutrinos. As a consequence, we expect (from MC) a  $\sim 50\%$  reduction of the up throughgoing muons with  $E_\mu \lesssim 10$  GeV, and only a  $\sim 20\%$  reduction for muons with  $E_\mu \gtrsim 10$  GeV.

Muons traversing MACRO are deflected by many small-angle scatters, the bulk of which are Coulomb scatterings from the nuclei and the atomic electrons (multiple Coulomb scattering). As an effect, relatively low energy up throughgoing muons are (slightly) deviated from a straight-line direction inside the detector. We evaluated that this deviation is of the order of few centimeters, up to  $E_\mu \sim 10$  GeV, and it exceed the intrinsic spatial resolution of the MACRO streamer tube cells.

A selection cut, based on the deviation of the muon sagitta from the straight line when the muon cross the whole detector, was defined. Each up throughgoing muon is classified as: *Low*= muon with a deviation from the straight line (from MC, lower energy muons with median  $E_\mu^{Low} = 11$  GeV); *High*= muon with no measurable deviation (muons with median energy  $E_\mu^{High} = 52$  GeV). The remaining events with ambiguous deviation, and which does not satisfy the high or the low energy cuts, were classified as *Medium*. From MC, they have an intermediate energy  $E_\mu^{Medium} = 33$  GeV. The same cuts were then applied to the simulated neutrino-induced events, and the results compared. To avoid systematic differences from data and MC, a detailed check of the detector simulation was performed. We used a large sample of measured and simulated downward going atmospheric muons, and we required that the distributions, used to define the selection cut, match together. The (preliminary) results are presented in Fig. 4. It is included also the point corresponding to the partially contained IU events. Only 87% of IU events have been induced

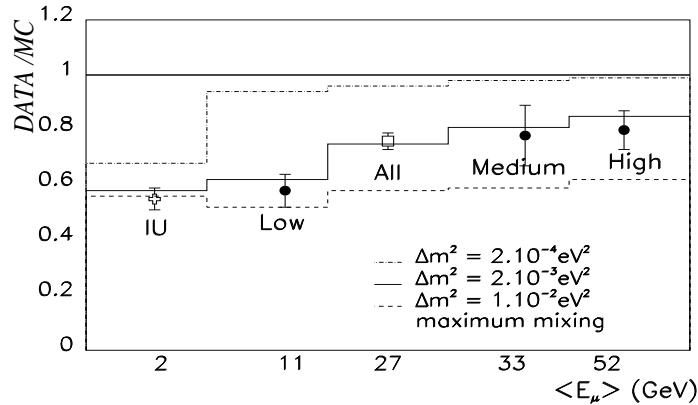


Figure 4: Ratio (detected events/expected events) vs. median muon energy for the whole sample of 723 up throughgoing muons (All), and for the sub sample with large (Low, 79 events) and small (High, 122 events) deviation from a straight line. It is also included the ratio for the events with intermediate energy (Medium, 49 events). The point IU corresponds to the 135 partially contained upgoing events. For all samples, the  $\nu_\mu$  path length is  $\sim 10^4$  km. The points are plotted with equal distance in abscissa, to guide the eye. The full line (data/MC=1) is the expectation without neutrino oscillations, for which a 17% total uncertainty is associated (25% for the IU point). The dashed lines are the expected reductions in case of  $\nu_\mu \rightarrow \nu_\tau$  oscillations with maximum mixing and three values of  $\Delta m^2$ .

by  $\nu_\mu$  CC interactions, the remaining by  $\nu_e$  and NC interactions.

Fig. 4 shows that lower energy events are more suppressed than higher energy ones. In a similar way, Fig. 2a shows that neutrinos with a longer path length are more suppressed; both effect are well explained by neutrino oscillation (eq. 1), with the oscillation parameter presented in Fig. 2b.

I acknowledge all the colleagues of the MACRO collaboration, in particular D. Bakari and Y. Becherini.

## References

- [1] S. Ahlen et al., Nucl. Instr. Meth. A324(1993)337.
- [2] M. Ambrosio et al., Phys. Lett. B434(1998)451;  
Phys. Lett. B357(1995)481.
- [3] M. Ambrosio et al., Phys. Lett. B478(2000)5;  
M. Spurio, Nucl.Phys.Proc.Suppl.85:37-43,2000 (hep-ex/9908066).
- [4] M. Ambrosio et al., Astropart. Phys. 9(1998)105.
- [5] F. Ronga, Nucl.Phys.Proc.Suppl.87:135,2000 (hep-ex/0001058), and references therein.
- [6] P. Lipari and M.Lusignoli, Phys. Rev. D57, 3842(1998).